



Distribution and properties of visceral nociceptive neurons in rabbit cingulate cortex

Robert W. Sikes^{a,*}, Leslie J. Vogt^b, Brent A. Vogt^b

^a Northeastern University, Department of Physical Therapy, 360 Huntington Avenue, Boston, MA 02115, USA

^b Cingulum NeuroSciences Institute and SUNY Upstate Medical University, 750 E. Adams Street, Syracuse, NY 13210, USA

Received 19 March 2007; received in revised form 18 July 2007; accepted 24 September 2007

Abstract

Human imaging localizes most visceral nociceptive responses to anterior cingulate cortex (ACC), however, imaging in conscious subjects cannot completely control anticipatory and reflexive activity or resolve neuron activity. This study overcame these shortcomings by recording individual neuron responses in 12 anesthetized and paralyzed rabbits to define the visceronociceptive response pattern by region and layer. Balloon distension was applied to the colon at innocuous (15 mmHg) or noxious (60 mmHg) intensities, and innocuous and noxious mechanical, thermal and electrical stimuli were applied to the skin. Simultaneous recording from multiple regions assured differences were not due to anesthesia and neuron responses were resolved by spike sorting using principal components analysis. Of the total 346 neurons, 48% were nociceptive; responding to noxious levels of visceral or cutaneous stimulation, or both. Visceronociceptive neurons were most frequent in ACC (39%) and midcingulate cortex (MCC, 36%) and infrequent in retrosplenial cortex (RSC, 12%). In contrast, cutaneous nociceptive units were higher in MCC (MCC, 43%; ACC, 32%; RSC, 23%). Visceral-specific neurons were proportionately more frequent in ACC (37%), while cutaneous-specific units predominated in RSC (62.5%). Visceral nociceptive response durations were longer than those for cutaneous responses. Postmortem analysis of electrode tracks confirmed regional designations, and laminar analysis found inhibitory responses mainly in superficial layers and excitatory in deep layers. Thus, cingulate visceral nociception extends beyond ACC, this is the first report of nociceptive activity in RSC including nociceptive cutaneous responses, and these regional differences require a new model of cingulate nociceptive processing.

© 2007 International Association for the Study of Pain. Published by Elsevier B.V. All rights reserved.

Keywords: Pain; Limbic cortex; Gastrointestinal tract; Sensory nociception; Neurophysiology; Neuroanatomy

1. Introduction

Human pain studies often activate cingulate cortex, however, the source of the nociceptive signal is poorly understood. Noxious stimulation with subtraction of innocuous activity shows regional differences by body tissue and response onset and duration. Becerra et al. [4] activated anterior midcingulate cortex (aMCC) and dorsal posterior cingulate cortex (dPCC) during innocuous and noxious heat and the latter habituated. Innocu-

ous thermal stimuli activated aMCC [24]; while noxious heat activated pMCC. Davis et al. [11] activated aMCC with noxious transcutaneous electrical median nerve stimulation but not innocuous stimulation and Büchel et al. [8] identified aMCC activity with a pain intensity function, while dorsal to this there was innocuous activation. Visceral distension frequently activates anterior cingulate cortex (ACC; Naliboff et al., 2001) and this site overlapped with anticipation of visceral pain. Indeed, anticipation of pain is associated with cingulate cortex [36,57]. Finally, noxious muscle stimuli activated MCC more rostrally than did noxious cutaneous stimuli [46,47] and C-fiber-generated second pain was associated with pregenual ACC [35].

* Corresponding author. Tel.: +1 617 373 5195; fax: +1 617 373 3161.

E-mail address: r.sikes@neu.edu (R.W. Sikes).

The cingulate premotor areas (CPMA) lie in the cingulate sulcus and are driven by noxious stimuli. Henderson et al. [18] showed intensity-coded, noxious muscle activation of the caudal CPMA. Self-paced, sequential finger opposition activated dorsal pMCC [24] and movement responses were in dorsal pMCC [8]. Finally, Moulton et al. [31] reported innocuous and noxious heat activity in dorsal pMCC, while dorsal aMCC was driven by noxious stimuli only. Large activations, however, preclude excitatory and inhibitory and laminar analyses and tight control of anticipation and reflexes.

Rabbit studies reported ACC neurons with large, bilateral cutaneous receptive fields and multimodal thermal and mechanical nociceptive responses of long duration [44]. Kuo and Yen [23] compared nociceptive responses in ACC with somatosensory cortex and reported longer duration responses in ACC and the same units in awake and chloralose-anesthetized animals had similar activity patterns, although baseline was reduced under anesthesia. This assures that neuron responses under anesthesia reflect nociceptive activity. There is only one study of ACC neuron responses during colorectal distension [15]. These neurons were not activated by innocuous distension and only 22% were nociceptive. Using gastrointestinal sensitization, they activated two times as many neurons with visceral distension and no changes in cutaneous driving suggesting some segregation of visceral and cutaneous afferents.

Problems inherent in conscious human research are resolved with anesthetized and paralyzed rabbits. Rabbit neurons are large and easily isolated for recording and its ACC, MCC, and retrosplenial cortex are well differentiated [52,55]. Here, the distribution of cingulate visceronociceptive neurons was evaluated along with the structure of each nociceptive layer and their excitatory and inhibitory characteristics. Simultaneous recordings in multiple regions negated the effects of fluctuating anesthetic and reflexes were blocked with pancuronium to assure pure sensory activity. The proportions of visceral and cutaneous nociceptive units were defined by region and layer.

2. Methods

2.1. Animal preparation

Twelve adult male New Zealand rabbits (3 to 4 kg) were used. They were initially anesthetized with a mixture of Nembutal and Xylazine (35 and 5 mg/kg) to allow insertion of a tracheal tube. The animal was then anesthetized for surgery with a mixture of Halothane (1.5–2%) and Oxygen (2 l/min, open system). Temperature was monitored and maintained at 37 °C with a circulating-water heating pad. The electrocardiogram was continuously monitored and recorded for later analysis (HP 78352a) and hydration was maintained by a saline drip into an ear vein.

The animal's head was fixed to the stereotaxic device by attaching a stainless steel bar to the cranium with skull screws and dental acrylic. Before hardening, the dental acrylic was molded into a well which was filled with sterile saline during the experiment. To minimize pulsation, small openings, approximately 2 by 5 mm, were made through the bone over target cortical areas, leaving the dura intact. Using Bregma as the reference, the anterior cingulate cortex (ACC) was explored from +4.0 to +7.0 MCC from +2.0 to –2.0 mm, and the retrosplenial cortex (RSC) from –4.0 to –6.0 mm [16,42].

After surgery, the anesthesia level was reduced to approximately 0.5% or until weak withdrawal reflexes could be elicited. At this experimental level of anesthesia, there were no spontaneous movements, and noxious cutaneous stimulation produced only short duration reflexive movements of the stimulated appendage with no coordinated movements of other limbs or any other signs of arousal. Noxious visceral stimulation produced an increase in abdominal tone and slow limb extension but no other movements. Additionally, heart rate was continuously monitored during the experiment to insure that noxious stimulation produced no increase in heart rate. This level of anesthesia is necessary for cortical responses to be elicited by noxious stimulation without producing arousal [44]. These procedures were approved by the Committee for the Humane Use of Animals, SUNY Upstate Medical University.

In 10 animals neuromuscular blockade was used to improve the stability of recordings. After the animal reached the experimental level of anesthesia, muscle tone and reflex movements were blocked with a single dose of neuromuscular blocking agent (Pancuronium bromide 2 mg/kg, i.v.), and the animal was artificially ventilated (Penlon Nuffield Ventilator Model 200 with Newton Valve, Abingdon, UK). Since reflexes cannot be monitored during neuromuscular blockade, withdrawal reflexes were carefully assessed before injection, and heart rate was continuously monitored throughout the period of paralysis ensuring that heart rate did not change in response to noxious stimulation. This blockade was effective for about 2 h at which time the level of anesthesia was reassessed before repeating the blockade. No animals showed signs of arousal after blockade. At the end of the recording session, the animal was deeply anesthetized with pentobarbital (40 mg/kg) and perfused with 4% paraformaldehyde for histology (see below).

2.2. Neuron recording

Cortical activity was recorded extracellularly as multiunit activity and resolved into individual neurons with spike sorting. Electrodes were varnish insulated sharpened tungsten wires (1–4 M Ω) in one of two configurations. In the first configuration, four individual electrodes were arranged in a single row spaced 200 μ m apart (Fred Haer, Inc., Bowdoin, ME; Matrix electrode). This electrode array was oriented to sample across cortical layers simultaneously as shown in Fig. 1b or along the anterior/posterior axis at some MCC and RSC sites. In the alternate configuration, two pairs of electrodes were spaced with one pair in MCC and the other in RSC to allow simultaneous recording in both regions. Thus, up to 8 electrodes could simultaneously record action potentials with 4

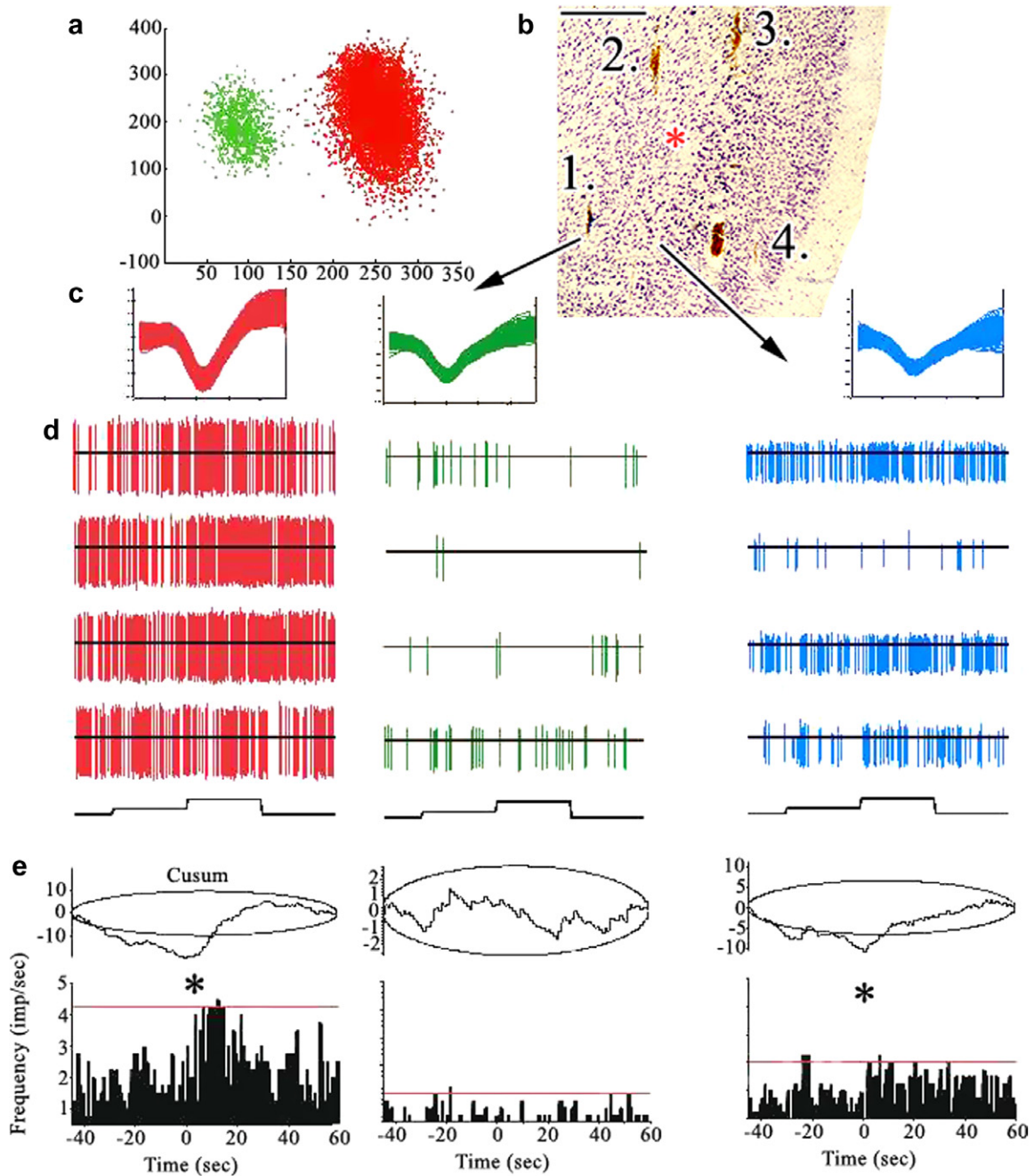


Fig. 1. Electrophysiological recording and electrode localization. (a) Principal components analysis of two units recorded from a single electrode (#1 in b). These units were differentiated with waveform characteristics shown in (c). A third unit was isolated simultaneously on electrode #2 (arrow drawn from the electrode tip). (b) Histological section showing four electrode tracks in area 32. The asterisk is the top of layer V and the calibration bar is for 500 μm. (d) Discharges of all three units during an innocuous and noxious colon distension. Action potentials during four successive trials are shown (each trial recorded simultaneously) and the period of innocuous and noxious stimulation is shown below (e). Cusum analysis and PSTHs for each discharge showing the first unit (red) had a strong response to noxious stimulation, the second (green) had no response, and the third (blue) had a variable but significant response to noxious visceral stimulation. Responses with significant Cusum, $p < 0.01$, are indicated by an asterisk.

electrodes spanning the cortical layers of ACC and the other four electrodes either placed at one posterior site or split between MCC and RSC. Action potentials detected at each electrode were fed into a multichannel amplifier and digitized at 40 kHz per channel (Plexon Inc, Dallas, TX – MAP system; Rasputin software). All waveforms that exceeded 3 times the baseline noise level were saved for spike sorting and subsequent offline analysis with a 600 μs spike window.

The electrode arrays were lowered through the intact dura mater until action potentials were first detected and then advanced into area 24b in ACC, area 24b' in MCC, and area 30 of RSC. Data from sites that postmortem histological analysis showed to be in area 8 were not included in the analysis. A series of cutaneous and visceral stimuli were applied (see below) and the electrode was then advanced to additional sites in 0.5 to 1.0 mm steps in ACC and 0.2 to 0.5 mm steps in MCC

and RSC. After each advance, the electrode was allowed to settle in the tissue for 15–30 min to improve stability. Search stimuli (see below) were applied, and if noxious responses were detected, the electrode position was slightly adjusted to better isolate the responsive units. The maximum depth explored was 5.0 mm in ACC and 2.0 mm at the posterior levels. Usually 3 or 4 sites were recorded on each probe, and 2 to 4 probes were made in each cortical area per animal. Probes were generally spaced 1.0 mm or more apart to assure postmortem identification of individual tracks.

A two step spike sorting approach was used to resolve the multi-unit waveforms recorded at each electrode into waveforms from single neurons (Plexon Inc., Offline Sorter software). After removal of electrical artifacts, waveforms were aligned to the maximum negative potential. Then 3D principal component analysis was used to identify waveform clusters and generate average waveform templates by automatic sorting methods with additional manual sorting when necessary. Template matching was then used to refine the sorting so that the resultant waveforms were statistically significantly different in principal component space (MANOVA, $p = 0.01$). An example of spike sorting with principal components analysis when more than one unit was identified on a single electrode is shown in Fig. 1a (electrode track #1). The waveform characteristics of each unit are also shown (C.) as well as their discharges generated by noxious stimulation as discussed below. A third unit recorded simultaneously but on a different electrode is also shown in the figure (electrode track #2). Autocorrelation interspike interval (ISI) histograms were examined to further insure that the waveforms represented separate neurons (e.g. no waveforms in cluster with $ISI < 1$ ms), and the stability of the waveform amplitude and shape was visually confirmed over the stimulation period. Finally, pair-wise statistical analysis was used to select units with statistically different waveform for inclusion. Simultaneously recorded units with different responses to noxious stimulation despite statistically overlapping clusters were also included in the sample population. Automatic sorting generally identified 2 to 5 clusters per electrode, and pair-wise analysis reduced this to about 2 units per electrode.

2.3. Response analysis

Analysis of peristimulus time histograms (PSTH) was used to identify neuronal responses to cutaneous and visceral stimulation. Cumulative summation analysis (Cusum; NeuroExplorer software, Nex Technologies, Littleton, MA) was used to assess the statistical significance of the response and improve the precision of response onset and offset measurements [10,40,45]. This method plots the cumulative sum of differences of PSTH bin count from the overall mean and constructs 99% confidence intervals to identify significant changes from the baseline activity. Individual sweeps were also examined for artifacts to make sure that the responses were reliably elicited.

Fig. 1 shows three typical unit responses recorded at a single site in area 24b of ACC. Two units from electrode #1 were recorded on the deepest of four electrodes, and the third unit was recorded on the adjacent electrode. Additionally, a second non-responsive unit on electrode #2 and single units, both non-responsive, were recorded on the more superficial elec-

trodes. Fig. 1a shows the principal component scatter plot for the first two units. The clusters were distinct and statistically significant ($p = 0.002$), and the waveforms of these two units were clearly different in amplitude when plotted (Fig. 1c). The responses of these units to visceral stimulation are shown in Fig. 1d and e. Action potentials are plotted in Fig. 1d along with a plot of innocuous and noxious visceral stimulation forces below. Four stimulation trials are shown. The first unit (red) shows a moderate but variable increase in firing after the onset of noxious visceral stimulation. The second unit (green) has a much lower spontaneous rate and shows no apparent response to stimulation. The third unit (blue) has an irregular firing pattern, but appears to modulate weakly with the noxious stimulation.

Statistical analysis of these responses is shown in Fig. 1e where the PSTH shows the excitatory response of the first unit more clearly, but there is much variability across the bins. Indeed, only one bin crosses the standard 99% PSTH confidence interval line (CI, red line) which would make classification of this response difficult. The more robust Cusum plot is less influenced by the irregularity of the firing rate and shows a clear change in firing just after the onset of noxious stimulation. Since this trend continues back into the 99% Cusum CI oval, the change in activity is statistically significant. In contrast, the Cusum plot of the second unit remains within the 99% CI oval and thus has no significant response to visceral stimulation. The PSTH for the third unit suggests a small increase in firing rate in PSTH but this is again obscured by irregular firing. Cusum analysis, however, more clearly shows a trend away from baseline and a significant increase in activity after the onset of noxious stimulation. The Cusum plot also facilitates the detection of the onset and offset of responses [13,34,45]. When a significant response was detected, the PSTH was replotted using a 0.1 s bin width to identify the bins corresponding to the beginning and end of the trend from baseline. Duration was the difference. This approach was again more robust than the standard 99% CI based on the t -statistic, especially when applied to irregular firing units and with a small number of trials.

2.4. Stimulation protocols

Visceral stimulation normally consisted of colorectal distention (CRD) at innocuous (15 mmHg) and noxious (60 mmHg) levels, while selected cases received higher noxious levels of stimulation (maximum 100 mmHg) to assure that a response was not being overlooked. The stimulation device consisted of a thin latex balloon or glove finger, approximately 5 cm long, sealed to a coupler which connected the stimulator through polyvinyl chloride tubing to a reservoir of water and allowed insertion of a thermal sensor into the stimulator for measuring rectal temperature. The reservoir was elevated to fixed heights to produce the desired amount of pressure. Elastic resistance in the latex was removed by filling the device with water and letting it sit for 30 min or more before insertion. The external 1 cm of the device was taped to limit perianal expansion. After checking for leaks under pressure, the device was inserted into the rectum and held in place by taping it to the tail. Pressure was continuously monitored using a low volume pressure transducer (Serta Systems, Natick, MA).

The standard stimulus application trial consisted of 30 s of colon distention at the innocuous pressure followed immediately by 30 s at a noxious pressure. All recording sites included in this study received at least 3 visceral stimulation trials. Most animals received 3–6 stimuli when a single level of noxious pressure was used or up to 9 when multiple levels were applied. After each visceral trial, no stimulation was applied for at least 3 min. Usually visceral trials alternated with cutaneous trials (see below) so the total time between visceral stimuli was 5 min or more.

Cutaneous stimulation generally followed the procedures previously described [44]. Two forms of cutaneous stimulation were routinely used; transcutaneous electrical (TCES) and mechanical pressure. TCES was tested at all sites and served as the initial search stimulus, since it does not damage tissue with repeated application. Stimuli were delivered by a bipolar surface electrode positioned across the shaved ear. Stimulation of the ipsilateral and contralateral ear was alternated. The standard current level was set at 6–10 mA and single pulses or trains of pulses (1 ms pulses at 100 Hz for 50 ms, 10 s ISI) were applied to test neuronal responses and, prior to muscle block, access anesthesia level. In some cases, lower levels of current were applied to evaluate threshold.

Qualitative mechanical pressure stimulation was applied at all sites included in this study. This consisted of a period of 5 or 10 s of innocuous mechanical pressure followed immediately by the same duration of noxious mechanical pressure. Innocuous pressure consisted of the application of blunt forceps to the ear or folds of skin and lightly brushing or squeezing the appendages. These stimuli, when applied to the investigators, evoked innocuous, light pressure sensations. Noxious levels of pressure consisted of stronger pinch of the ear, folds of skin or appendages with sharp forceps to the point that elicited withdrawal. When applied to the investigator, these stimuli were sharply noxious but did not persist more than a few seconds after termination. Since these stimuli can damage tissue with repeated application, stimulation sites were marked and spaced at least 1 cm apart. During each cutaneous trial, both contralateral and ipsilateral sites were tested. Whenever possible, the presence of whole body nociceptive receptive fields [44] was confirmed by stimulating ears, neck, back and all four limbs. The number of cutaneous stimuli ranged from 3 to 15 trials with interstimulus intervals of 2 min or more. In some cases, calibrated mechanical stimuli were applied with a spring-loaded device with a pair of 1 mm probes that contacted the skin. Pressure was controlled by compression of the spring to fixed lengths calibrated in 2 Newton steps to a maximum of 8 Newtons. When applied to the investigators, the pain threshold was 3–4 Newtons and the highest level was strongly noxious. Stimulation consisted of 5 or 10 s of innocuous stimulation followed by the same interval of noxious stimulation. Finally, some rabbits received stimulations including thermal stimuli applied with a probe (3 mm diameter) and heated by a Peltier device to 40–60 °C.

2.5. Statistical analysis

Units were classified as nociceptive if they showed a statistically significant change in firing rate during the application of noxious stimulation when compared to application of

innocuous stimuli (Cusum analysis). There were two main categories of nociceptive neurons: visceronociceptive and cutaneous nociceptive. These classes overlap, since some units respond to both modes of noxious stimulation. Therefore, nociceptive units were further classified into visceral only, cutaneous only, and viscerocutaneous units. Additionally, responses were classified as excitatory or inhibitory based on an initial increase or decrease in firing rate following noxious stimulation.

χ^2 analysis (SPSS Crosstab analysis, $p < 0.05$) was used to determine if the three regions of cingulate cortex differed in proportions of units within these categories. Statistical differences between regions and response classifications in mean onset and duration were determined with analysis of variance (SPSS Univariate GLM analysis, $p < 0.05$) with post hoc pairwise comparisons (SPSS Bonferroni $p < 0.05$) and data plots were made with Neuroexplorer (Nex Technologies) or Matlab (Mathworks, Natick, MA).

2.6. Histological preparations and localization of electrodes, areas, and layers

Following cardiac perfusion with about 500 ml of cold 0.9% saline and about 1000 ml of 4% paraformaldehyde in phosphate buffered saline, brains were removed to the same fixative for several days and then transferred through a series of 10%, 20% and 30% buffered sucrose until they sank. Sections were cut at 40 μ m and stained with thionin (3 min; 0.05% in 3.7% sodium acetate, 3.5% glacial acetic acid, pH 4.5) for histological localization of the electrode tracks. In two animals, alternate sections were processed for neuron-specific nuclear binding protein (NeuN) and two control cases that received no surgical procedures were also prepared for NeuN immunohistochemistry. These sections were washed in phosphate-buffered saline (PBS), incubated in primary antibody in PBS (1:1000 dilution, mouse; Chemicon, Temecula, CA) containing 0.3% Triton X-100 and 0.5 mg/ml bovine serum albumin (BSA) overnight at 4 °C. Sections were rinsed in PBS and incubated in biotinylated secondary antibody at 1:200 in PBS/Triton X-100/BSA for 1 h. Following rinses in PBS, sections were incubated in ABC solution (1:4; Vector Labs, Burlingame, CA) in PBS/Triton X-100/BSA for 1 h followed by PBS rinses and incubation in 0.05% diaminobenzidine, 0.01% H₂O₂ in a 1:10 dilution of PBS for 5 min. Sections were rinsed in PBS and mounted, air-dried and counterstained with thionin, dehydrated and coverslipped.

To allow multiple uses of the electrode arrays, electrolytic lesions were not made at the end of each penetration. The multiple parallel tracks of the array electrodes allowed sufficient localization of the recording sites along the anteroposterior (y) and mediolateral (x) axes. Site depths from the dorsal surface were estimated by plotting stereotaxic coordinates of the sites relative to the coordinates of the first recorded units in layers II–III on the histologically reconstructed track. Given the large spacing of recording sites, this method allowed accurate determination of the cytoarchitectural region of recording sites.

To determine the location of electrodes in the superficial versus deep layers, the paths of individual tracks at each stereotaxic site were traced as they passed through superficial layers II–IV or deep layers V and VI. Since there was some

uncertainly on the precise depth of the site from the dorsal surface, only track paths that stayed within a layer for at least 1 mm above and below the estimated site location were included in the laminar analysis. An example of a histological case stained with thionin and immunoreacted for NeuN is shown in Fig. 2. Two tracks were located in layer Va of area 32 (Fig. 2b; 1 and 2). Even during the short period of electrical recording, a glial response can be detected by the thionin-stained glia along the track interspersed with the NeuN-immunoreacted neurons.

The cytoarchitecture of cingulate cortex has been reported for Nissl-stained material [55] and the first report of midcingulate cortex (MCC) in the rabbit made with Nissl-stained preparations [52]. The ACC had the greatest density of cutaneous nociceptive neurons in rabbit [44] and MCC is the most active region during noxious stimulation in human [54]. Since both of these regions and RSC were analyzed in this report, a series of five microphotographs are presented at levels marked with asterisks in the right hemisphere in Fig. 2a. Two levels of ACC (Fig. 2c) MCC (Fig. 2d) and a rostral one through RSC (Fig. 2e) show the layers and architecture of each area in the control hemisphere; i.e., the one not used for neuronal recording. The red asterisk in each photograph marks the top of layer Va and it represents the border between superficial and deep layers. As noted in Fig. 2b, area 32 has a very thin layer IV (also termed dysgranular) and two electrode tracks

were identified in layer Va of this area. Simultaneous recordings from MCC and RSC were made in this case as discussed further below.

A crucial difference between rabbits/rats and primates occurs in the posterior part of cingulate cortex. The cortical surface in the former species is comprised of RSC, while that in the latter is area 23 and 31. In primates, the RSC is entirely enclosed within the callosal sulcus. Thus, rats and rabbits do not have a posterior cingulate gyrus *per se*, while primates have such a gyrus and it is comprised of RSC in the callosal sulcus and posterior cingulate cortex on the gyral surface. These comparative differences have been discussed in detail [60].

In contrast to area 32, area 24 does not have a layer IV. A few key differences between area 24b in ACC and area 24b' in MCC along the rostrocaudal axis include the following: (a) progressive reduction in neuron density associated with larger neuron sizes, (b) progressively larger neurons in layers Va and Vb, (c) progressively thicker layer VI comprised of very small and granular appearing neurons. Comparison of RSC area 29c and 30 shows them to be very distinct as in rodents [60]. Area 30 was the most frequently sampled site in RSC in this study, and compared to area 29c, it has broad layers II and III, a thin (dysgranular) layer IV, very large neurons in layer Va, a relatively neuron-free layer Vb, and a broad layer VI with small neurons.

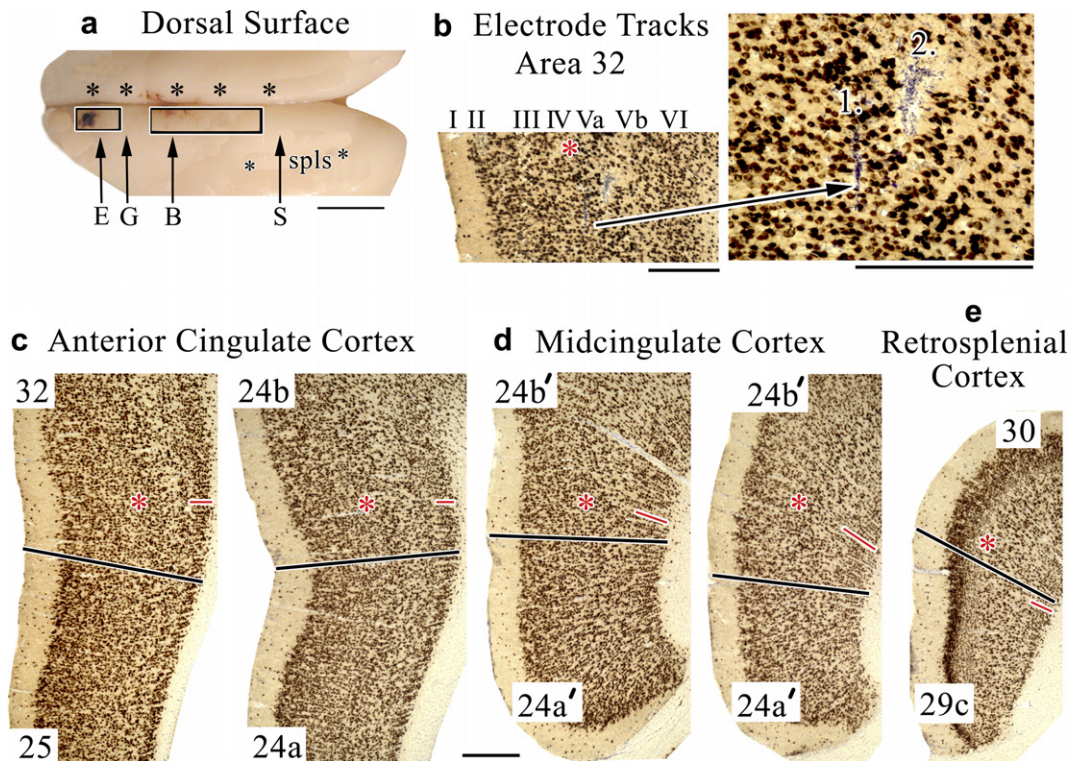


Fig. 2. Immunohistochemical assessment of electrode tracks, areas and layers. (a) Dorsal surface with the recording trenches (boxes) shown overlying the left hemisphere where simultaneous recordings were made from each region as shown in Fig. 4. The 5 asterisks on the right hemisphere locate where the photographs of normal cortex were taken below (c–e). The level as “E” is that for the electrode tracks shown in (b). The splenium of the corpus callosum is at level “S” and the splenial sulcus (spls) is shown with two asterisks in the left hemisphere. “G” and “B” levels refer to the genu of the corpus callosum and bregma, respectively. Calibration bar 5 mm. (b) Electrode tracks shown in layer Va of area 32. The red asterisk is at the border between layers IV and Va in this section, between layers III and Va in other ACC and MCC areas, and between layers IV and Va in area 30 (e). All histological calibration bars are 500 μm.

3. Results

3.1. Nociceptive responses in cingulate cortex regions

The responses of 346 neurons were recorded in cingulate cortex, and 166 neurons or 48% showed a significant response to visceral and/or cutaneous noxious stimulation. The overall percentages of nociceptive units were similar across regions (Table 1) with a somewhat larger proportion found in MCC (57.2%) and ACC (50.9%) while 32.4% of RSC responses were nociceptive. The proportions differed significantly by region, however, when the mode of stimulation was included in the analysis. Overall, noxious visceral stimulation elicited responses in 32.7% of nociceptive neurons, and noxious cutaneous stimulation produced responses in 31.8%. Significantly more visceronociceptive responses were observed in ACC and MCC (38.9% and 35.7%, respectively), while only 12.2% of RSC neurons responded to visceral stimulation. The percentages of cutaneous nociceptive neurons were highest in MCC (42.9% vs 31.9% in ACC and 23% in RSC), but differences were not statistically significant ($\chi^2 p = 0.055$). Units in all areas had cutaneous nociceptive receptive fields that encompassed the entire body with no noticeable difference between sides. No reliable response was observed to innocuous levels of visceral or cutaneous stimulation during these trials.

3.2. Subclasses of nociceptive responses

Nociceptive responses were grouped into three categories; (a) visceral only with a significant response to noxious visceral stimulation and no response to cutaneous stimulation, (b) viscerocutaneous with responses to both visceral and cutaneous noxious stimulation and (c) cutaneous only with significant responses exclusively to cutaneous noxious stimulation (Table 2). Overall, the 166 nociceptive units were distributed into these categories in approximately equal numbers (Visceral Only 33.7%, Viscerocutaneous 34.3% and Cutaneous Only 31.9%).

There were significant differences in the response sub-modalities through cingulate cortex as also shown in Table 2. In ACC, 37.3% of the neurons responded exclusively to visceral stimulation, while 39.1% of them were

viscerocutaneous. Only 22.6% of ACC neurons responded exclusively to cutaneous stimulation. In contrast, MCC units responded best to cutaneous noxious stimulation with 37.5% responding exclusively to these stimuli, while 37.5% responded to both. Noxious visceral only responses were observed in only 25% of MCC nociceptive units. The distribution of responses in RSC had a much higher proportion of cutaneous only responses and very few viscerocutaneous responses. Most RSC units responded exclusively to cutaneous stimulation (62.5%), while 29.2% (7 of 24) responded exclusively to visceral stimulation, and only 8.3% (2 of 24) had a viscerocutaneous nociceptive response.

Typical examples from the three categories of nociceptive responses in the cingulate cortex regions are shown in Fig. 3. The ACC visceral only example unit (Fig. 3-1) shows a strong excitatory response to the onset of noxious visceral stimulation (latency 5.8 s; duration 22 s) and no response to cutaneous stimulation. The viscerocutaneous response (Fig. 3-2) shows a longer latency visceral nociceptive excitation (latency 13.6 s; duration 18.7 s) and has a less vigorous but significant response to cutaneous nociceptive stimulation with a shorter onset (latency 7.6, duration 11.3). The cutaneous only response (Fig. 3-3) has a short latency, moderate response to cutaneous stimuli (latency 1.1 s; duration 10.8 s). While a slight increase in firing rate can be seen following visceral noxious stimulation in this unit, this increase was not significantly different from baseline.

In MCC the excitatory visceral only nociceptive responses were similar to those in ACC. The example response in Fig. 3-1 has a moderate increase to visceral nociceptive stimulation (latency 4.8 s; duration 17.9 s) and no response to cutaneous stimulation. In contrast to ACC where most viscerocutaneous responses were excitatory to both types of stimulation, half of the MCC viscerocutaneous neurons had an inhibitory response to visceral stimulation and an excitatory response to cutaneous stimulation (Fig. 3-2). The example unit showed strong and very long duration inhibition to noxious visceral stimulation (latency 3.2 s; duration 132.2 s). The response to noxious cutaneous stimulation shows a fast early excitation peak followed by an extended period of increased activity (latency 0.6 s; total duration 17.9 s). The cutaneous only unit (Fig. 3-3)

Table 1
Nociceptive responses in cingulate regions

Response type	ACC	MCC	RSC	Total
Nociceptive ^a	50.9% (96/216)	57.2% (32/56)	32.4% (23/74)	48.0% (166/346)
Visceronociceptive ^a	38.9% (84/216)	35.7% (20/56)	12.2% (9/74)	32.7% (113/346)
Cutaneous nociceptive ^b	31.9% (69/216)	42.9% (24/56)	23.0% (17/74)	31.8% (110/346)

Percentage total and count of units for each response within each cingulate region.

^a Significant difference, χ^2 , $p < 0.05$.

^b Not significant, χ^2 , $p = 0.055$.

Table 2
Nociceptive response subtypes by region

Nociceptive subtype	ACC	MCC	RSC	Total
Visceral only	37.3% (41/110)	25.0% (8/32)	29.2% (7/24)	33.7% (56/166)
Viscerocutaneous	39.1% (43/110)	37.5% (12/32)	8.3% (2/24)	34.3% 57/166)
Cutaneous only	22.6% (23/110)	37.5% (12/32)	62.5% (14/24)	31.9% 53/166)

Percentage total and count of units for each subtype within each region.
 χ^2 contingency table analysis, $p = 0.002$ significant difference between regions.

shows a similar short latency onset with an early peak followed by a lower level of excitation (latency 0.3 s; total duration 5.0 s) but no significant response to visceral stimulation.

Visceral responses in RSC were infrequent, weaker than in ACC and MCC, and inhibitory responses predominated (see below). The visceral only response

shown in Fig. 3-1 shows a weak but significant decrease in firing (latency 5.0 s; duration 47.2 s) following visceral noxious stimulation with no response to cutaneous stimulation. The visceral response in the viscerocutaneous example unit (Fig. 3-2) shows a weak long-duration inhibition to both visceral and cutaneous stimulation (visceral latency 8.8 s, duration 77.8 s; cutaneous latency

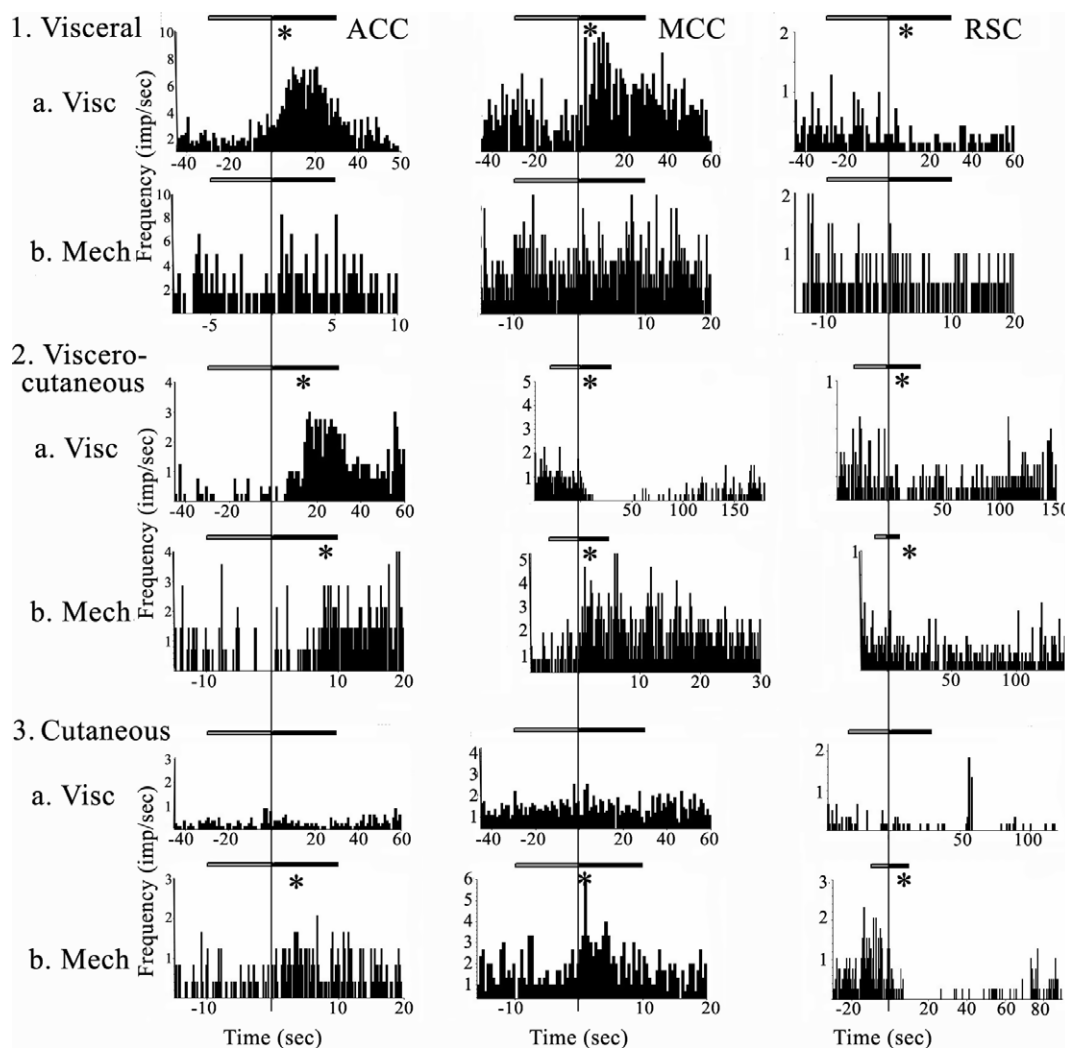


Fig. 3. Examples of neuron responses in each cingulate region. (1) Visceral only, (2) viscerocutaneous and (3) cutaneous only responses in each of the cingulate regions; ACC, MCC and RSC. Each PSTH accumulates all trials of (a). Visceral (Visc) and (b). Mechanical (Mech) cutaneous stimulation for each neuron and were evaluated for a significant response by Cusum analysis (PSTHs with responses significant at $p < 0.01$ are indicated by an asterisk). The bar at each response indicates the duration of innocuous (clear) and noxious (shaded) stimulation. Time scales are adjusted to match noxious stimulation onset for each neuron and when necessary expanded to show long duration responses clearly. Visceral responses predominate in ACC, while cutaneous responses are more prevalent in MCC and RSC.

16.6 s, duration 117.8 s). The most vigorous type of noxious response in RSC was the cutaneous only response (Fig. 3-3). This neuron shows strong inhibition to noxious cutaneous stimulation (latency 1.8; duration 73.2) and no response to visceral stimulation.

3.3. Simultaneous recordings in all regions

Comparison of separately recorded units in a number of animals can generate differences that are associated with a variable level of anesthesia and this always raises doubts as to the fundamental differences among response properties. For this reason, recordings were made in two or three regions simultaneously and an example of these observations is shown in Fig. 4.

The ACC site is located in area 32 as shown in Fig. 2b; 5 mm rostral to bregma and at a 2 mm depth. The MCC unit was in area 24b'; 1 mm rostral to bregma and at a 1.2 mm depth, while the RSC unit was located in area 30; 5 mm caudal to bregma and at a 0.2 mm depth. The ACC unit was a visceral only unit with a strong response to noxious visceral stimulation (latency 2.6 s; duration 16.6 s) and no significant response to innocuous or noxious cutaneous stimulation. The MCC example shows a viscerocutaneous response. Noxious stimulation produced moderate visceral (latency

10.6 s; duration 20.4 s) and cutaneous (latency 0.6 s; duration 6.2 s) responses. The nociceptive response in RSC was cutaneous only. The cutaneous noxious stimulation produced a small but significant increase over baseline (latency 3.0 s; duration 5.8 s), while visceral noxious did not increase firing over baseline. All double and triple region recordings confirmed the distribution of subclass response properties observed in single penetration recordings, and thus it was reasonable to combine data from each region for statistical analysis.

3.4. Distribution of excitatory and inhibitory responses

While excitatory and inhibitory responses were elicited by both visceral and cutaneous noxious stimulation, cingulate regions differed significantly in the proportion of these response properties (Table 3). In ACC, visceronociceptive excitatory responses predominated (67.9%). In MCC, similar proportions of excitatory and inhibitory responses were observed (55% vs 45%), while in RSC visceronociceptive responses were far more likely to be inhibitory (77.8%). Cutaneous nociceptive responses were primarily excitatory in all regions (ACC, 88.4%; MCC, 79.2%; RSC, 58.8%).

The majority of nociceptive responses showed a single excitatory or inhibitory period following stimulation.

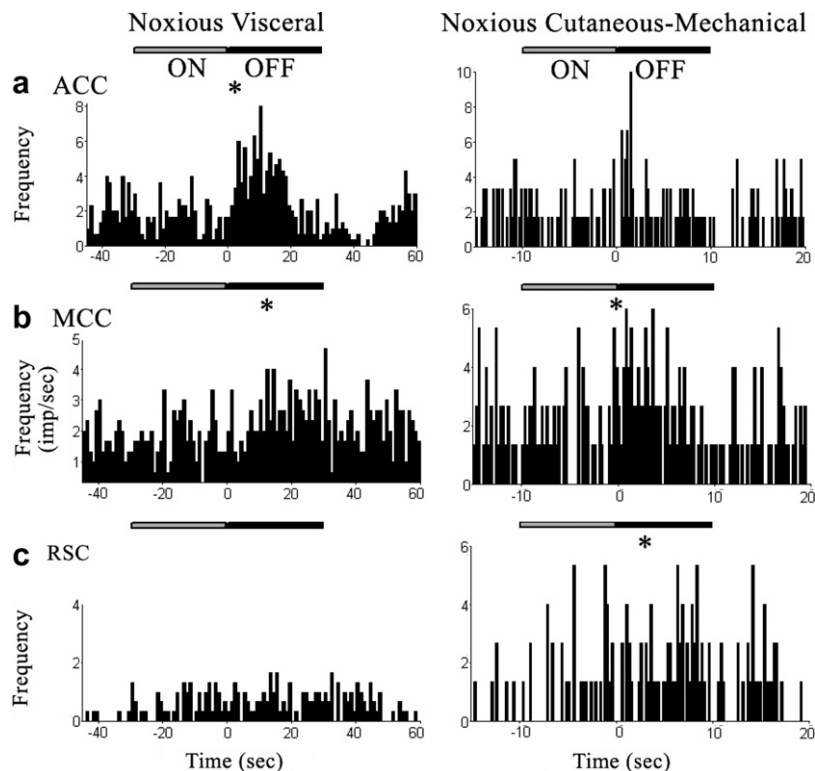


Fig. 4. Simultaneous recordings from neurons in each cingulate region. Each column of PSTHs was simultaneously recorded with three different electrodes during visceral and cutaneous stimulation (asterisk, significant response; Cusum $p < 0.01$). The onset and offset of innocuous (clear) and noxious (shaded) stimuli are marked with a bar above each response. The shift from prominent visceral drive in ACC to prominent cutaneous drive in RSC is apparent and, therefore, cannot be attributed to variations in the level of anesthesia.

Table 3
Distribution of excitatory and inhibitory responses

Nociceptive type	Response	ACC	MCC	RSC
<i>Visceronociceptive</i>				
	Excitatory	67.9% (57 of 84)	55.0% (11 of 20)	22.2% (2 of 9)
	Inhibitory	32.1% (27 of 84)	45.0% (9 of 20)	77.8% (7 of 9)
<i>Cutaneous Nociceptive</i>				
	Excitatory	88.4% (61 of 69)	79.2% (19 of 24)	58.8% (10 of 17)
	Inhibitory	11.6% (8 of 69)	20.8% (5 of 24)	41.2% (7 of 17)

χ^2 – visceronociceptive $p = 0.022$, cutaneous nociceptive $p = 0.017$.

A small percentage, however, had a biphasic response, primarily in ACC where 6 of 84 visceronociceptive units had an initial excitatory response followed by an inhibitory period (4 units) or a second excitatory period (2 units). In contrast, only 1 of 20 MCC units and none of the RSC units showed biphasic visceronociceptive responses. For cutaneous nociceptive responses, 5 of 69 ACC units had biphasic excitatory responses with the second excitation associated with the stimulus offset – an on/off response. This was also observed in 1 of 24 MCC units and 2 of 17 RSC units.

Most viscerocutaneous units had the same response to visceral and cutaneous noxious stimulation (75.4%), but in MCC 50% of the viscerocutaneous units (6 of 12 units) had an inhibitory response to visceral stimulation and an excitatory response to cutaneous stimulation (see Fig. 3). In ACC, this response mismatch occurred in only 18.6% of the viscerocutaneous units (8 of 43 units) and in neither of the two RSC viscerocutaneous units. Analysis of ACC and MCC viscerocutaneous responses by response type did not, however, show a significant difference (χ^2 , $p = 0.110$).

3.5. Response latency and duration

Visceral response latencies were longer than cutaneous response latencies in all cingulate regions as shown in Table 4. The response duration was also longer, however, this may reflect the difference in stimulus duration (30 s for visceral and 5 to 10 s for cutaneous). It should be noted that response duration matched stimulus duration in ACC and MCC better than in RSC and that

cutaneous response duration was significantly longer in RSC at 35.9 s than in ACC and MCC (14.6 and 10.7 s, respectively).

Additional regional distinctions were revealed when the excitatory or inhibitory nature of the responses was factored into the analysis (Table 5). Overall, inhibitory responses had significantly longer duration than excitatory responses; 53.7 s vs. 20.3 s for visceral and 46.8 s vs. 10.5 s for cutaneous noxious stimulation. Furthermore, cutaneous inhibitory response duration was significantly longer in RSC than in ACC and MCC (63.8 s vs. ACC 43.8 s and MCC 28.0 s), while the excitatory response duration was similar across regions. Response onset did not significantly differ between excitatory and inhibitory responses or between the cingulate regions.

3.6. Deep and superficial neuron responses

Most units that could be definitively assigned to the superficial or deep layers were in ACC (ACC, 61 units; MCC, 5 units; RSC, 20 units). Furthermore, due to sampling bias in RSC only 4 of the 20 units were located in the deep layers. Therefore only data from ACC were further analyzed for statistically significant laminar response differences. Of the 5 units that were localized to specific layers in MCC, 3 had nociceptive responses. Two superficial units were both viscerocutaneous and showed an excitatory response to cutaneous stimulation and an inhibitory response to visceral noxious stimulation (location of one of these units is shown in Fig. 5 and the response in Fig. 3). A deep layer unit had an

Table 4
Response onset and duration by region and stimulus

Stimulus	ACC	MCC	RSC
<i>Visceral, initial response</i>			
Onset	5.7 ± 0.95 (N = 84)	5.2 ± 0.75 (N = 19)	6.1 ± 1.72 (N = 9)
Duration	31.2 ± 3.08 (N = 84)	34.9 ± 7.26 (N = 19)	47.3 ± 5.93 (N = 9)
<i>Cutaneous, initial response</i>			
Onset	2.3 ± 0.30 (N = 69)	1.7 ± 0.47 (N = 19)	2.9 ± 1.46 (N = 5)
Duration ^a	14.6 ± 2.43 (N = 69)	10.7 ± 2.57 (N = 24)	35.9 ± 9.54 (N = 17)

Mean ± standard error of mean.

^a Significant difference between regions, one-way ANOVA $p < 0.05$.

Table 5
Excitatory and inhibitory onset and durations by region and stimulus

Response	ACC	MCC	RSC	Total
<i>Visceral excitatory resp.</i>				
Onset	4.0 ± 1.04 (N = 57)	4.2 ± 1.23 (N = 10)	5.7 ± 5.45 (N = 2)	4.1 ± 0.88 (N = 69)
Duration	20.8 ± 1.73 (N = 57)	15.2 ± 3.38 (N = 10)	30.1 ± 5.50 (N = 2)	20.3 ± 1.54 (N = 69) ^a
<i>Visceral inhibitory resp.</i>				
Onset	9.2 ± 1.84 (N = 27)	6.2 ± 0.71 (N = 9)	6.2 ± 1.90 (N = 7)	8.1 ± 1.21 (N = 43)
Duration	53.1 ± 7.31 (N = 27)	56.9 ± 11.02 (N = 9)	52.2 ± 6.38 (N = 7)	53.7 ± 5.16 (N = 43) ^a
<i>Cutaneous excitatory resp.</i>				
Onset	2.1 ± 1.56 (N = 61)	1.7 ± 1.43 (N = 19)	5.0 ± 2.15 (N = 10)	2.3 ± 0.30 (N = 90)
Duration	10.8 ± 1.69 (N = 61)	6.2 ± 1.02 (N = 19)	16.4 ± 6.11 (N = 10)	10.5 ± 1.36 (N = 90) ^b
<i>Cutaneous inhibitory resp.</i>				
Onset	3.8 ± 0.93 (N = 8)	2.9 ± 1.46 (N = 5)	4.2 ± 2.08 (N = 7)	3.7 ± 0.85 (N = 20)
Duration	43.8 ± 13.08 (N = 8) ^c	28.0 ± 8.43 (N = 5) ^c	63.8 ± 16.98 (N = 7) ^c	46.8 ± 8.43 (N = 20) ^b

Mean ± standard error of mean.

^a Visceral duration significantly different between excitatory and inhibitory responses, ANOVA $p < 0.001$.

^b Cutaneous duration significantly different between excitatory and inhibitory responses, ANOVA $p < 0.001$.

^c Cutaneous duration significantly different between regions, ANOVA $p < 0.005$.

excitatory response to only cutaneous stimulation (Fig. 3-3). Of the 20 units in RSC, only 4 responded to noxious stimulation. Three of these were located in superficial layers where one cutaneous only unit had an excitatory response to noxious stimulation (shown in Fig. 4). The other superficial units were viscerocutaneous and were inhibited by both forms of stimulation (one shown in Fig. 3-3). Finally, the deep layer unit (location shown in Fig. 5 and response in Fig. 3-1) was visceral only with a weak, but significant, inhibition.

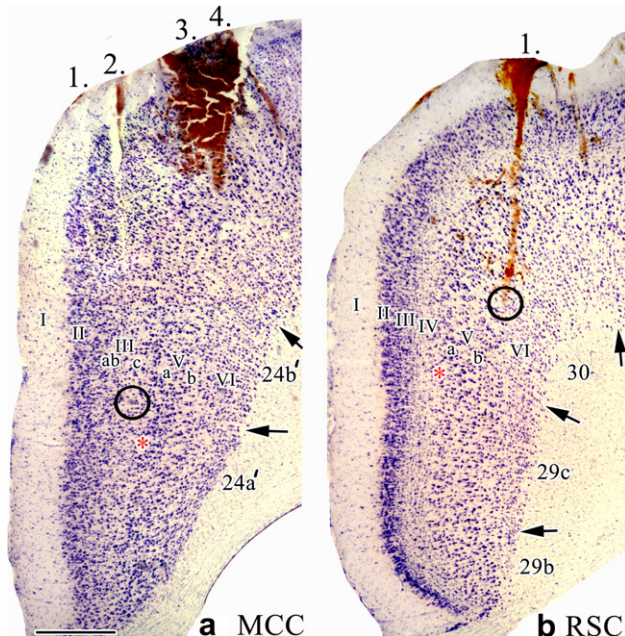


Fig. 5. Recording sites in MCC and RSC for units in the circles showing the high resolution of localization in tissue stained with thionin. (a) Cutaneous Only unit shown in Fig. 3 located in layer IIIc. (b) Visceral Only inhibitory response shown in Fig. 3 located at the junction of layers V and VI in area 30.

In ACC, no significant difference was noted between superficial versus deep units in the proportion of nociceptive units; 63.2% (12 of 19) of superficial and 61.9% (26 of 42) of deep units responding to noxious visceral and/or cutaneous stimulation. Restricting the analysis to visceral and cutaneous nociceptive responses also revealed no differences. Of superficial units, 47.4% (9 of 19) were visceronociceptive and 36.8% (7 of 19) were cutaneous nociceptive. The deep units had similar proportions with 45.2% (19 of 42) visceronociceptive and 38.1% (16 of 42) cutaneous nociceptive. Also, no distinction could be made in terms of the modality of the responses with similar proportions of visceral only, viscerocutaneous and cutaneous only responses in each layer as shown in Table 6.

Laminar differences were seen when the excitatory or inhibitory nature of the response was contrasted. Many units in the superficial layers (66.7%; 6 of 9 units) showed inhibition to noxious visceral stimulation (Table 6). In contrast units in the deep layers were mainly excited by noxious visceral stimulation (78.9%; 15 of 19) and this difference was significant. A similar tendency was observed with cutaneous nociceptive responses (Table 6), although the difference was not significant (Fisher Exact Test, $p = 0.067$).

While the response onset to visceral noxious stimulation was similar between layers (mean ± standard error, 2.5 ± 3.5 s superficial versus 4.2 ± 2.4 s deep) the duration of responses was significantly different between superficial units (38.3 ± 6.3 s) and deep units (19.4 ± 2.7 s; $p = 0.02$). Cutaneous nociceptive responses showed this pattern to be reversed, but the mean differences were not significant. For onset the means were 4.0 ± 1.3 s for superficial and 2.2 ± 0.6 s for deep units, while the durations were 11.1 ± 2.7 s for superficial and 22.1 ± 9.0 s for deep units.

Table 6
Superficial and deep nociceptive responses in ACC

Nociceptive response type	Superficial layers	Deep layers
<i>All units</i>		
Nociceptive	63.2% (12 of 19)	61.9% (26 of 42)
Visceronociceptive	47.4% (9 of 19)	45.2% (19 of 42)
Cutaneous nociceptive	36.8% (7 of 19)	38.1% (16 of 42)
<i>Nociceptive units categories</i>		
Visceral only	41.7% (5 of 12)	38.5% (10 of 26)
Visceral & cutaneous	33.3% (4 of 12)	34.6% (9 of 26)
Cutaneous only	25.0% (3 of 12)	26.9% (7 of 26)
<i>Visceronociceptive responses^a</i>		
Excitatory	33.3% (3 of 9)	78.9% (15 of 19)
Inhibitory	66.7% (6 of 9)	21.1% (4 of 19)
<i>Cutaneous nociceptive responses</i>		
Excitatory	57.1.1% (4 of 7)	93.8% (15 of 16)
Inhibitory	42.9% (3 of 7)	6.2% (1 of 16)

Percentage total and count of units for each nociceptive response type are shown.

^a Significant difference, Fischer Exact Test $p < 0.05$, response type by layer.

4. Discussion

4.1. Nociception extends beyond anterior cingulate cortex

Affect is often attributed to ACC based on studies of pain unpleasantness [22], anticipation of pain [36], and reliance on Brodmann's cingulate dichotomy. Since pain evoked-potential studies suggest short-latency activation in dPCC [5,25,39] and there is a low level of emotion-relevant activation here [53,54], nociceptive activity in pMCC and dPCC is not likely affective. Since the rabbit and rat do not have a dPCC, dorsal RSC may perform similar functions in these species. The present study reports single-neuron, visceronociceptive activity throughout cingulate cortex and for the first time in RSC. The visceral and viscerocutaneous units have a topographic pattern with most in ACC (76.4%), fewer in MCC (62.5%), and fewest in RSC (37.5%), while cutaneous-only nociceptive neurons were twice as frequent as visceral-only nociceptive neurons in RSC (23% vs 12.2%, respectively) and this was not the case for ACC (38.9% vs 31.9%, respectively). Thus, the caudal limit of ACC cannot be based on where the nociceptive signal is observed.

The conundrum of nociceptive activity in caudal cingulate cortex can be addressed with the midcingulate concept. This concept emphasizes the response selection, skeletomotor, and body orientation in space functions of cingulate cortex, the CPMA and motor projections of this region [52,54]. The nociceptive signals in MCC and RSC are not relevant to affect *per se* but rather to premotor orientation of the body and head to noxious stimulation. A premotor model of cingulate pain processing emphasizes body orientation and movement selection in these regions [59].

4.2. Source and latency of visceral nociceptive signal

Visceral nociceptive signals enter the forebrain via the dorsal column to the ventral posterolateral nucleus [14,19,20] and spinal and brainstem afferents to the midline and intralaminar thalamic nuclei (MITN; [1,53]). Nociceptive afferents to ACC do not appear to arise from the anterior insula because there are no such projections in rabbit [55], they are weak in monkey [28,56], and undercut lesions that remove cortical inputs to ACC do not block nociception [44], while thalamic lidocaine does. Thus, the thalamus is a source of nociceptive cingulate inputs during premotor functions beyond simple emotions and unpleasantness.

The latency of visceral responses in cingulate cortex (4–6 s onset) was longer than those to cutaneous responses and their duration lasted one minute or more. Long-duration, viscerocutaneous responses are of interest because they are more likely to contribute to cingulate plasticities such as paired-pulse facilitation [48] than are very brief responses such as those of cutaneous origin. Long-latency and sustained short-latency responses to colorectal distension last as long as two minutes [33] and Ammons et al. [1] reported biphasic responses to electrical stimulation of cardiopulmonary inputs to centrolateral neurons with onsets of 6 and 51 ms for some units again lasting over a minute. Thus, response durations may indicate a more prominent role of visceral inputs to cingulate plasticities than for cutaneous responses.

Viscerocutaneous nociceptive responses may be explained by thalamic afferents that drive cingulate cortex. The midline and intralaminar thalamic nuclei contain nociceptive neurons [9,12] and receive spinothalamic input including the reuniens, parafascicular (Pf) and periventricular nuclei [27]. Ammons et al. [1] showed that viscerocutaneous spinothalamic tract neurons project to the medial thalamus including the parafascicular and centrolateral nuclei and these nuclei receive input from the pronociceptive subnucleus reticularis dorsalis [51] as does the parabrachial nucleus [7]. Both of these latter nuclei respond to visceral and cutaneous nociceptive stimulation [37,50]. Thus, non-somatopic, viscerocutaneous nociception in ACC derives from spinal cord, subnucleus reticularis dorsalis and parabrachial nuclei via the MITN.

Although the source of viscerocutaneous afferents likely arises in the MITN, the problem of cutaneous-only and visceral-only responses originates from present findings and those of Gao et al. [15] showing visceral hypersensitization with increased baseline activity and lowered threshold for visceral activation in ACC that were not associated with changes in noxious cutaneous responses. Although it is not known how independent channels process cutaneous-only and visceral-only pain in cingulate cortex, the following possibilities are relevant.

In terms of cutaneous-only processing, such input could arise from nucleus cuneatus projections to Pf and reuniens if this channel remained selective [51]. Along the same line, there may be some thalamic nuclei that receive preferential cutaneous input and do not project to ACC but do project to MCC and dorsal PCC. Thalamic projections following small retrograde tracer injections in rabbit cortex suggest candidates for a cutaneous nociceptive pathway [61]. Inputs from nociceptive nuclei to rostral RSC (area 29d/30) arise from the central, controlateral, submedial, and parvocellular mediodorsal nuclei, while in the monkey, the nucleus limitans projects to dPCC [43,56]. Some nuclei, such as the paraventricular nucleus that are known to receive spinothalamic afferents [27], have not yet been evaluated for nociceptive processing and could also have a cutaneous selectivity. It is also possible that posterior sensory association cortices that project to RSC and MCC contribute to such signals and were not evaluated in lesion studies [44]. Finally, visceral-only nociceptive responses could result from a cortical circuit interaction such as cutaneous inhibitory responses that negate excitatory ones. There are presently no circuitries available whereby each cingulate area processes nociceptive information.

4.3. Role of superficial and deep layers in nociception

There is a significant difference in the laminar distribution of visceral nociceptive neurons, responses were mainly excitatory in deep and inhibitory in superficial layers, and there was a regional shift with excitatory responses mainly in ACC and inhibitory ones in RSC. Finally, the inhibitory responses were always longest (64 s in RSC). In ACC, visceral and cutaneous noxious responses were primarily excitatory, but laminar analysis showed that deep layer neurons were mainly excited and superficial neurons inhibited. Although few neurons in RSC were localized by layer, visceral inhibition in MCC and RSC was observed mainly in superficial layers, while noxious cutaneous stimulation produced excitation.

Laminar projections of cingulate cortex include three classes and laminar differences in nociceptive responses may impact pain processing accordingly. First, layer VI and some layer V neurons project to the thalamus [6,21]. Second, layer V projects to the periaqueductal gray [2,26,32], the caudate nucleus [38], and parabrachial nucleus [63]. These projections regulate the descending noxious inhibitory system [41,49]. Third, layer II–III neurons emit corticocortical projections [3,55] and suggest further integration preceding descending outputs.

Monconduit et al. [30] showed that somatosensory layer VI gates the flow of noxious information to the cortex. GABA_A receptor agonists in layer VI enhanced innocuous processing in the ventral posterolateral thalamic nucleus, while GABA_A antagonists enhanced pro-

cessing of nociceptive signals. Layer VI may be engaged in similar functions in cingulate cortex and differences in the structure of layer VI are notable (Fig. 2): ACC has a thin layer VI but large neurons; MCC has smaller neurons but thick layer VI; RSC has a thin layer VI but small neurons. Finally, Yamamura et al. [62] evaluated nociceptive deep layer neurons in rat area 32 (not area 24 as reported) and showed them to be mainly large pyramids with excitatory responses.

4.4. Cingulate premotor areas are nociceptive

Sulcal cingulate cortex contains the CPMA and this subregion has been explored for links to pain processing. Thalamic projections to ACC were first proposed to have a role in pain behaviors rather than pain perception *per se* [58] and Hatanaka et al. [17] showed a high proportion of Pf neurons projecting to the rostral CPMA. A cingulate premotor pain model with an output motor processing stage has been proposed [59]. Henderson et al. [18] showed intensity-coded activation of the caudal CPMA by noxious muscle stimulation and Moulton et al. [31] reported innocuous and noxious heat activation of dorsal pMCC, while dorsal aMCC was driven by noxious stimuli only; regions that contain CPMA. In contrast to primates, rodents and lagomorphs do not have a cingulate sulcus or two cingulate premotor areas, they have a single CPMA to regulate both skeletomotor and autonomic functions. Corticospinal projections in rat arise mainly from pregenual area 32 [29]. This area overlaps with autonomic control cortex (Neafsey et al., 1993) and the cutaneous nociceptive site reported in rabbits [44] and assures direct nociceptive regulation of premotor outputs as in primates.

Acknowledgement

This work was supported by NIH NINDS Grant RO1 NS44222.

References

- [1] Ammons WS, Girardot M-N, Foreman RD. T₂–T₅ spinothalamic neurons projecting to medial thalamus with viscerosomatic input. *J Neurophysiol* 1985;54:73–89.
- [2] An X, Bandler R, Öngür D, Price JL. Prefrontal cortical projections to longitudinal columns in the midbrain periaqueductal gray in macaque monkeys. *J Comp Neurol* 1998;401:455–79.
- [3] Bassett LJ, Berger TW. Associational connections between the anterior and posterior cingulate gyrus in rabbit. *Brain Res* 1992;248:371–416.
- [4] Becerra LR, Breiter HC, Stojanovic M, Fishman S, Edwards A, Comite AR, et al. Human brain activation under controlled thermal stimulation and habituation to noxious heat: an fMRI study. *Mag Res Med* 1999;41:1044–57.
- [5] Bentley DE, Derbyshire SWG, Youell PD, Jones AKP. Caudal cingulate involvement in pain processing: an inter-individual laser

- evoked potential source localization study using realistic head models. *Pain* 2003;102:265–71.
- [6] Berger TW, Milner TA, Swanson GW, Lynch GS, Thompson RF. Reciprocal anatomical connections between anterior thalamus and cingulate-retrosplenial cortex in the rabbit. *Brain Res* 1980;201:411–7.
- [7] Bester H, Bourgeois L, Villanueva L, Besson J-M, Bernard J-F. Differential projections to the intralaminar and gustatory thalamus from the parabrachial area: a PHA-L study in the rat. *J Comp Neurol* 1999;405:421–49.
- [8] Büchel C, Bornhövd K, Quante M, Glauche V, Bromm B, Weiller C. Dissociable neural responses related to pain intensity, stimulus intensity, and stimulus awareness within the anterior cingulate cortex: a parametric single-trial laser functional magnetic resonance imaging study. *J Neurosci* 2002;22:970–6.
- [9] Casey KL. Unit analysis of nociceptive mechanisms in the thalamus of the awake squirrel monkey. *J Neurophysiol* 1966;29:727–50.
- [10] Davey NJ, Ellaway PH, Stein RB. Statistical limits for detecting change in the cumulative sum derivative of the peristimulus time histogram. *J Neurosci Methods* 1986;17:153–66.
- [11] Davis KD, Taylor SJ, Crwaley AP, Wood ML, Mikulis DJ. Functional MRI of pain- and attention-related activations in the human cingulate cortex. *J Neurophysiol* 1997;77:3370–80.
- [12] Dong WK, Ryu H, Wagman IH. Nociceptive responses of neurons in medial thalamus and their relationship to spinothalamic pathways. *J Neurophysiol* 1978;41:1592–613.
- [13] Ellaway PH. Cumulative sum technique and its application to the analysis of peristimulus time histograms. *Electroencephalogr Clin Neurophysiol* 1978;45:302–4.
- [14] Foreman RD, Blair RW, Weber RN. Viscerosomatic convergence onto T2–T4 spinoreticular, spinoreticular–spinothalamic, and spinothalamic tract neurons in the cat. *Exp Neurol* 1984;85:597–619.
- [15] Gao J, Wu X, Owyang C, Li Y. Enhanced responses of the anterior cingulate cortex neurons to colonic distension in viscerally hypersensitive rats. *J Physiol* 2006;570.1:169–83.
- [16] Girgis M, Shih-Chang W. New stereotaxic atlas of the rabbit brain. *WH Green: St. Louis*; 1985.
- [17] Hatanaka N, Tokuno H, Hamada I, Inase M, Ito Y, Imanishi M, et al. Thalamocortical and intracortical connections of monkey cingulate motor areas. *J Comp Neurol* 2003;462:121–38.
- [18] Henderson LA, Bandler R, Gandevia SC, Macefield VG. Distinct forebrain activity patterns during deep versus superficial pain. *Pain* 2006;120:286–96.
- [19] Hobbs SF, Chandler MJ, Bolser DC, Foreman RD. Segmental organization of visceral and somatic input onto C₃–T₆ spinothalamic tract cells of the monkey. *J Neurophysiol* 1992;68:1575–90.
- [20] Houghton AK, Wanf C-C, Westlund KN. Do nociceptive signals from the pancreas travel in the dorsal column? *Pain* 2001;89:207–20.
- [21] Kaitz SS, Robertson RT. Thalamic connections with limbic cortex. II. Corticothalamic projections. *J Comp Neurol* 1981;195:527–45.
- [22] Kulkarni B, Bentley DE, Elliott R, Youell P, Watson A, Derbyshire SWG, et al. Attention to pain localization and unpleasantness discriminates the functions of the medial and lateral pain systems. *Eur J Neurosci* 2005;21:3133–42.
- [23] Kuo C-C, Yen C-T. Comparison of anterior cingulate and primary somatosensory neuronal responses to noxious laser-heat stimuli in conscious, behaving rats. *J Neurophysiol* 2005;94:1825–36.
- [24] Kwan CL, Crawley AP, Mikulis DJ, Davis KD. An fMRI study of the anterior cingulate cortex and surrounding medial wall activations evoked by noxious cutaneous heat and cold stimuli. *Pain* 2000;85:359–74.
- [25] Lenz FA, Rios M, Zirh A, Chau D, Krauss G, Lesser RP. Painful stimuli evoke potentials recorded over the human anterior cingulate gyrus. *J Neurophysiol* 1998;79:2231–4.
- [26] Mantyh PW. Forebrain projections to the periaqueductal gray in the monkey, with observations in the cat and rat. *J Comp Neurol* 1982;206:146–58.
- [27] Mantyh PW. The terminations of the spinothalamic tract in the cat. *Neurosci Lett* 1983;38:119–24.
- [28] Mesulam M-M, Mufson EJ. Insula of the old world monkey. III. Efferent cortical output and comments on its function. *J Comp Neurol* 1982;212:38–52.
- [29] Miller MW. The origin of corticospinal projection neurons in rat. *Exp Brain Res* 1987;67:339–51.
- [30] Monconduit L, Lopez-Avila A, Molat J-L, Chalus M, Villanueva L. Corticofugal output from the primary somatosensory cortex selectively modulates innocuous and noxious inputs in the rat spinothalamic system. *J Neurosci* 2006;26:8441–50.
- [31] Moulton EA, Keaser ML, Gullapalli RP, Greenspan JD. Regional intensive and temporal patterns of functional MRI activation distinguishing noxious and innocuous contact heat. *J Neurophysiol* 2005;93:2183–93.
- [32] Neafsey EJ, Hurley-Gius KM, Arvanitis D. The topographical organization of neurons in the rat medial frontal, insular and olfactory cortex projecting to the solitary nucleus, olfactory bulb, periaqueductal gray and superior colliculus. *Brain Res* 1986;377:261–70.
- [33] Ness TJ, Gebhart GF. Characterization of neuronal responses to noxious visceral and somatic stimuli in the medial lumbosacral spinal cord of the rat. *J Neurophysiol* 1987;57:1867–92.
- [34] Oliver E, Baker SN, Nakajima K, Brochier T, Lemon RN. Investigation into non-monosynaptic corticospinal excitation of macaque upper limb single motor units. *J Neurophysiol* 2001;86:1573–86.
- [35] Ploner M, Gross J, Timmermann L, Schnitzler A. Cortical representation of first and second pain sensation in humans. *Proc Natl Acad Sci USA* 2002;99:12444–8.
- [36] Porro CA, Baraldi P, Pagnoni G, Serafini M, Facchin P, Maieron M, et al. Does anticipation of pain affect cortical nociceptive systems? *J Neurosci* 2002;22:3206–14.
- [37] Roy J-C, Bing Z, Villanueva L, Le Bars D. Convergence of visceral and somatic inputs onto subnucleus reticularis dorsalis neurons in the rat medulla. *J Physiol* 1992;458:235–46.
- [38] Royce GJ. Cells of origin of corticothalamic projections upon the centromedian and parafascicular nuclei in the cat. *Brain Res* 1983;258:11–21.
- [39] Schlereth T, Baumgärtner U, Magerl W, Stoeter P, Treede R-D. Left-hemisphere dominance in early nociceptive processing in the human parasyllvian cortex. *NeuroImage* 2003;20:441–54.
- [40] Scutter SD, Türker KS. Muscle spindle afferent input to motoneurons in human masseter. *J Neurophysiol* 1999;82:505–7.
- [41] Senapati AK, Lagraize SC, Huntington PJ, Wilson HD, Fuchs PN, Peng YB. Electrical stimulation of the anterior cingulate cortex reduces responses of rat dorsal horn neurons to mechanical stimuli. *J Neurophysiol* 2005;94:845–51.
- [42] Shek JW, Wen GY, Wisniewski HM. Atlas of the rabbit brain and spinal cord. *Basel*: Karger; 1986.
- [43] Shibata H, Yukiie M. Differential thalamic connections of the posteroventral and dorsal posterior cingulate gyrus in the monkey. *Eur J Neurosci* 2003;18:1615–26.
- [44] Sikes RW, Vogt BA. Nociceptive neurons in area 24 of rabbit cingulate cortex. *J Neurophysiol* 1992;68:1720–31.
- [45] Smith HC, Davey NJ, Savic GD, Maskill W, Ellaway PH, Jamous MA, et al. Modulation of single motor unit discharges using magnetic stimulation of the motor cortex in incomplete spinal cord injury. *J Neurol Neurosurg Psychiatry* 2000;68:516–20.
- [46] Strigo IA, Duncan GH, Boivin M, Bushnell MC. Differentiation of visceral and cutaneous pain in the human brain. *J Neurophysiol* 2003;89:3294–303.

- [47] Svensson P, Minoshima S, Beydoun A, Morrow TJ, Casey KL. Cerebral processing of acute skin and muscle pain in humans. *J Neurophysiol* 1997;78:450–60.
- [48] Sylantsev SO, Lee C-M, Shyu B-C. A parametric assessment of GABA antagonist on paired-pulse facilitation in the rat anterior cingulate cortex. *Neurosci Res* 2005;52:362–70.
- [49] Toda K. Anterior cingulate-induced inhibition of activities of descending periaqueductal gray matter neurons in rats. *Pain Res* 1992;7:71–9.
- [50] Villanueva L, Bing Z, Bouhassira D, Le Bars D. Encoding of electrical, thermal, and mechanical noxious stimuli by subnucleus reticularis dorsalis neurons in the rat medulla. *J Neurophysiol* 1989;61:391–402.
- [51] Villanueva L, Desbois C, Le Bars D, Bernard J-F. Organization of diencephalic projections from the medullary subnucleus reticularis dorsalis and the adjacent cuneate nucleus: a retrograde and anterograde tracer study in the rat. *J Comp Neurol* 1998;390:133–60.
- [52] Vogt BA. Structural organization of cingulate cortex: Areas, neurons, and somatodendritic transmitter receptors. In: Vogt BA, Gabriel M, editors. *Neurobiology of cingulate cortex and limbic thalamus*. Boston: Birkhäuser; 1993. p. 19–70.
- [53] Vogt BA. Pain and emotion interactions in subregions of the cingulate gyrus. *Nat Rev Neurosci* 2005;6:533–44.
- [54] Vogt BA, Berger GR, Derbyshire SWJ. Structural and Functional dichotomy of human midcingulate cortex. *Eur J Neurosci* 2003;18:3134–44.
- [55] Vogt BA, Sikes RW, Swadlow HA, Weyand TG. Rabbit cingulate cortex: Cytoarchitecture, physiological border with visual cortex and afferent cortical connections including those of visual, motor, postsubicular and transcingulate origin. *J Comp Neurol* 1986;248:74–94.
- [56] Vogt BA, Pandya DN, Rosene DL. Cingulate cortex of rhesus monkey I. Cytoarchitecture and thalamic afferents. *J Comp Neurol* 1987;262:256–70.
- [57] Vogt BA, Porro CA, Faymonville M-E. Pain processing and modulation in the cingulate gyrus. In: Fluor H, Kalso E, Dostrovsky JO, editors. *Proceedings of the International Association for the Study of Pain, Chapter 36*. Seattle: IASP Press; 2006. p. 415–30.
- [58] Vogt BA, Rosene DL, Pandya DN. Thalamic and cortical afferents differentiate anterior from posterior cingulate cortex in the monkey. *Science* 1979;204:205–7.
- [59] Vogt BA, Sikes RW. Cingulate nociceptive circuitry and roles in pain processing: the cingulate premotor pain model. In: BA Vogt (ed) *Cingulate Neurobiology and Disease*, Oxford University Press; Oxford 2008; in press.
- [60] Vogt BA, Vogt LJ, Farber NB. Cingulate cortex and models of disease. In: Paxinos G (ed), *The Rat Nervous System*, third edition. 2004, Chapter 22, 705–727.
- [61] Vogt LJ, Vogt BA, Sikes RW. The limbic thalamus in rabbit: architecture, projections to cingulate cortex and distribution of muscarinic acetylcholine, GABA and opioid receptors. *J Comp Neurol* 1992;319:205–17.
- [62] Yamamura H, Iwata K, Tsuboi Y, Toda K, Kitajima K, Shimizu N, et al. Morphological and electrophysiological properties of ACCx nociceptive neurons in rat. *Brain Res* 1996;735:83–92.
- [63] Yasui Y, Itoh K, Takada M, Mitasvni A, Kaneko T, Mizuno N. Direct projections to the parabrachial nucleus in the cat. *J Comp Neurol* 1985;234:77–86.